A Tissue Oxygenation Sensor and an active in-vitro phantom for sensor validation

Ching-Mei Chen, *Member, IEEE*, Richard M. Kwasnicki, Vincenzo F. Curto, Guang-Zhong Yang, *Fellow IEEE and* Benny P.L. Lo, *Senior Member, IEEE*

***Abstract*— A Free Flap is a tissue reconstruction procedure where healthy tissue is harvested to cover up vital structures after wound debridement. Microvascular anastomoses are carried out to join the arteries and veins of the flap with recipient vessels near the target site. Continuous monitoring is required to identify flap failure and enable early intervention to salvage the flap. Although there are medical instruments which can assist surgeons in monitoring flap viability, high upfront costs and time-consuming data interpretation has hindered the use of such technologies in practice. Surgeons still rely largely on clinical examination to monitor flaps after operations. This paper presents a low cost, low power (6.6mW) and miniaturized Hamlyn StO_2 (tissue oxygen saturation) sensor which can be embodied as a plaster and attached to a flap for real-time monitoring. Similar to the design of oxygen saturation (SpO_2/SaO_2) sensors, the Hamlyn StO_2 sensor was designed based on photoplethysmography (PPG), but with a different target of quantifying tissue perfusion rather than capturing pulsatile flow. To understand spectral response to oxygenation/deoxygenation and vascular flow, an active *in-vitro* silicone phantom was developed. The new sensor was validated using the silicone phantom and compared with a commercially available photospectroscopy and laser Doppler machine (O2C, LEA, Germany). In addition, *in-vivo* experiments were conducted using a brachial pressure cuff forearm ischemia model. The experiment results have shown a high correlation between the proposed sensor and the O2C machine ($r=0.672$, $p<0.001$), demonstrating the potential value of the proposed low cost sensor in post-operative free flap monitoring.**

***Index Terms* — Photoplethysmography, PPG, StO_2, SpO_2/SaO_2, Tissue Oxygen Saturation, free flap monitoring, silicone skin phantom.**

Ching-Mei Chen was with the Hamlyn Centre Imperial College London, UK, and she is now with Department of Engineering Science, University of Oxford, UK (ching-mei.chen@eng.ox.ac.uk).

Richard M. Kwasnicki is with the Department of Surgery Cancer, Imperial College London, UK (richard.kwasnicki07@imperial.ac.uk)

Vincenzo F. Curto was with the Hamlyn Centre Imperial College London, and he is now with Department of Engineering, University of Cambridge, UK (vfc23@eng.cam.ac.uk).

Guang-Zhong Yang and Benny P L. Lo are with the Hamlyn Centre, Imperial College London (email: {g.z.yang, benny.lo} @imperial.ac.uk).

I. INTRODUCTION

FOLLOWING the rapid advances in microelectronics, sensing and wireless technologies, many new wearable and implantable Body Sensor Network (BSN) devices and systems have been proposed, which has led to the development of new applications and research areas [1-3]. It is anticipated that the low cost pervasive sensing technologies could potentially reduce the workload of healthcare professionals, improve the quality of care and patient outcomes, and facilitate the transformation of the current healthcare service from a reactive approach to a proactive care model [4].

The post-operative care of patients after soft tissue reconstruction is one of the scenarios where BSN technologies could help to relieve the extensive human resources required for the intensive monitoring of tissue viability and enable early intervention. Free autologous tissue transfer is a surgical technique often used to reconstruct a defect where no other technique is suitable after wound debridement or tumor resection. Free flap reconstruction is commonly used in the treatment of severe lower limb fractures [5] and increasingly being applied in breast reconstruction [6]. Unlike skin grafts or local tissue flaps where original blood supply to the grafts/flaps are retained, the tissue flap has to be completely removed from the donor site, and reattached it to the target site along with its artery and vein to recipient vessels. As such, the efficacy of the circulation through the vasculature of the tissue flap determines the survival of the flap, and therefore, the success of the soft tissue reconstruction. The microvascular anastomoses are vulnerable to complications including blood clotting inside the vessels, twisting, kinking or compression of the vessels in the new location. Venous thrombosis is a common cause of flap failure which accounts for up to 20% of all free flap reconstruction failures [7]. Early detection of flap failure could significantly improve the chances of salvaging the tissue flap and prevent the need to harvest an additional flap, which is costly both to the patient's health and economically.

Surgeons have sought a reliable and objective flap monitoring device for several decades. An ideal free flap monitoring device "*should be harmless to patient and flap, rapidly responsive, accurate, reliable, and applicable to all types of flap* " as outlined by Creech and Miller in 1975 [8]. Since then, different technological approaches and devices have been proposed and piloted for free flap monitoring [9]. For example, the Transcutaneous Oxygen pressure ($TcpO_2$) Near-

Infrared Spectroscopy (NIRS), laser Doppler flowmetry and tissue spectrophotometry have all be used for monitoring tissue flaps.

$TcpO_2$ measures the oxygen tension in the skin by inducing local hyperemia (by heating the skin tissue to ~45°C using electrodes) and allowing oxygen to flow freely to the skin, and the oxygen pressure is then measured on the skin surface [10, 11]. $TcpO_2$ has been widely used for assessing wound healing, determining the level of amputation for patients with diabetic foot ulcers [12] and evaluating tissue perfusion of patients in intensive care [13].

By detecting the variation of blood hemoglobin concentration, NIRS has been widely used for capturing peripheral blood flow and neural activity [14, 15]. NIRS has also been used to measure regional tissue oxygen saturation [16], and studies have found that NIRS can be used to estimate the survival rate of patients after traumatic shock by measuring the oxygen saturation on the thenar eminence [17].

A more established approach in flap monitoring is to combine laser Doppler flowmetry and tissue spectrophotometry to analyze superficial oxygen saturation of hemoglobin on the skin surface and oxygen supply in skeletal muscles [18, 19]. Although some of these technologies have demonstrated the ability to detect flap failure and lead to improved patient outcomes [20-23], the adoption of these technologies in clinical practice is limited. This is mainly due to the high up-front cost, complexity in set up, bulkiness of the system, false alarms and time consuming and complex data interpretation.

A miniaturized StO_2 [24] was developed based on the reflective photoplethysmography (PPG) approach [25] with the aim of enabling pervasive and continuous monitoring of tissue viability after soft tissue reconstruction,. Fig. 1 shows the Hamlyn StO_2 sensor with its dimensions. To validate the sensor, comparative studies were conducted comparing the Hamlyn StO_2 sensor with standard instruments using a tissue phantom and a healthy subject pressure cuff ischemia model. The key contributions of this paper include (1) introducing a StO_2 sensor using PPG technology for tissue perfusion measurements; (2) assessing the sensor response with respect to the color of the blood using an active *in-vitro* phantom; (3) applying a forearm ischemia model to evaluate the feasibly and reliability of the sensor in monitoring tissue flaps. Results are compared with NIRS and laser Doppler – OC2 as tissue oxygen saturation reading and blood flow information references in our lab. The following section describes the design methodologies of the Hamlyn StO_2 sensor, active *in-vitro* phantom and the ischemia model. Results and statistical analysis are presented in section III, follow by conclusion and discussion.

II. METHODS

A. *StO_2 Sensor Node Design*

The design of the low power Hamlyn StO_2 sensor is extended from our previous work on the reflective PPG sensor with noise removal using a time division multiplexing method [25]. Instead of focusing on motion artefact removal and capturing peripheral pulse waves, the new sensor is redesigned considering the signal attenuation in tissue, optimal wavelength, and signal-to-noise ratio for measuring tissue oxygenation.

As tissue flaps often have less hemoglobin in the tissue and led to low saturation readings, typical $Sp(a)O_2$ (SpO_2/SaO_2) sensor with Light Emitter Diode (LED) pairs of 660nm/940nm will fail to accurately measure in such low saturation range (i.e. <70%), as these wavelengths are mainly sensitive in the high saturation range of 70-100% [26]. As stated in [26], there is a strong correlation between perturbed and baseline of modulation ratio from arterial oxygen saturation readings by replacing a pair of LEDs from 660nm/940nm to 735nm/890nm in both Monte Carlo (MD) and Photon Diffusion (PD) models. As such, two LEDs with closer wavelengths of 740nm and 880nm were chosen for the StO_2 sensor development [24]. To calibrate the sensor, an 805nm LED was used, as this wavelength is closer to the isosbestic point of deoxygenated hemoglobin and oxygenated hemoglobin curves.

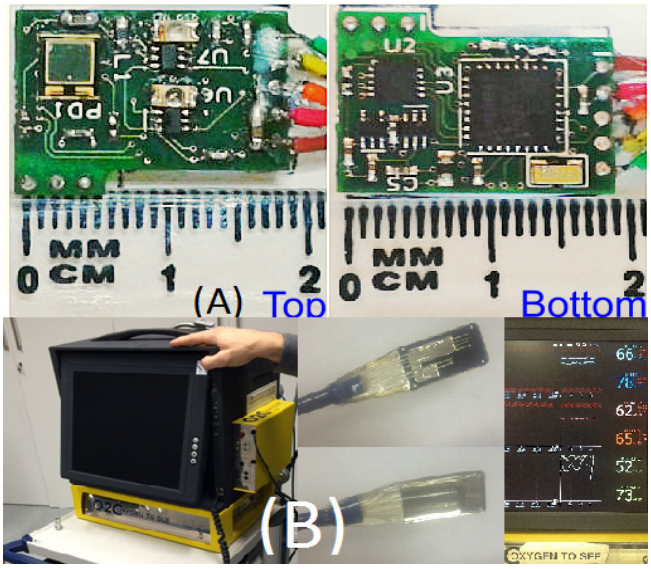

Fig. 1 (A) The Hamlyn StO2 sensor (B) PC-based oxygen-to-see (O2C) [19]

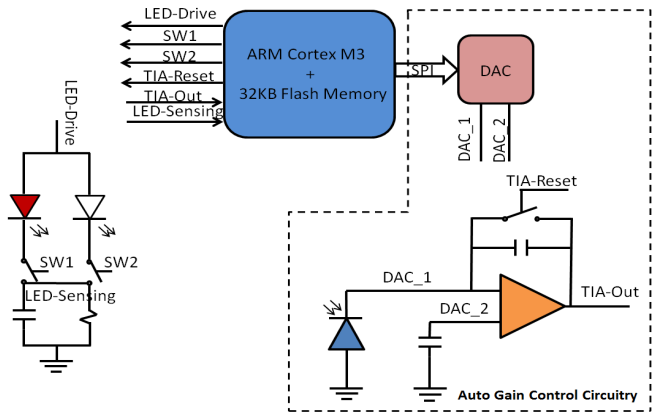

Fig. 2 The system diagram of the Hamlyn StO_2 sensor

The Hamlyn StO_2 sensor uses an EFM32TG210 ARM Cortex ultra-low power core which drives the LEDs and takes measurements from the phototransistors via the DAC (digital analog converter) to adjust reference voltages at two inputs of operational amplifier, so that the sensor can be adjusted and adapted to different skin tones. The output of the amplifier is connected to one of the 12 bit ADC inputs of the chip, as depicted in Fig. 2. The average power consumption of the sensor is 6.6mW with a sampling rate of 1 KHz.

Table 1 lists the tissue absorption and scattering constants used for the sensor design. The table is summarized from [27] where μ_a represents the sum total of arterial/venous blood and absorption of bloodless tissue, $\mu's$ is the scattering constant in different wavelengths. *HHb* and O_2Hb are deoxygenated hemoglobin and oxygenated hemoglobin of tissue concentration.

TABLE 1 TISSUE ABSORPTION AND SCATTERING CONSTANTS [27]

Coefficient	Wavelength		
(mm^{-1})	735nm	805nm	890nm
μ_a *bloodless tissue*	0.008	0.008	0.007
HHb	0.616	0.373	0.393
O_2Hb	0.178	0.38	0.549
$\mu's$	1.22	1.05	0.89

A healthy subject study was conducted to determine the ratio correction for hardware calibration, and a pair of LEDs with wavelengths of 805nm and 880nm was used in the study. Raw sensor data was then obtained from a healthy subject and readings of *HHb* and O_2Hb at 805nm were found to be slightly different from the corresponding constants as listed on Table 1 with hardware ratio correction r=0.95. As the sensor used is of similar wavelengths as per [27], the correlation between the signals was found to be very high, but due to manufacturing differences, it was found that a small correction ratio r was needed to calibrate the sensor. Distance between the photodiode and LEDs were adjusted in a range of 7.2mm to 7.4mm to obtain optimal readings in the reflective mode.

After the hardware ratio correction r was obtained, *HHb* and O_2Hb values were then derived for the Hamlyn StO_2 sensor's LEDs (with wavelengths of 740nm and 880nm) from Eq. 1-3 below [24]. The μ_a bloodless tissue coefficient is neglected, as the difference is only 0.001 between the two wavelengths.

$$805\,(nm) = HHb + 1.02\,O_2Hb \times r \quad (1)$$

$$740\,(nm) = 1.65\,HHb + 0.468\,O_2Hb \times r \quad (2)$$

$$880\,(nm) = 1.05\,HHb + 1.44\,O_2Hb \times r \quad (3)$$

A final tissue oxygen saturation (StO_2) in percentage is then calculated by,

$$S_tO_2(\%) = \left(\frac{O_2H_b}{O_2H_b + HH_b}\right) * 100\% \quad (4)$$

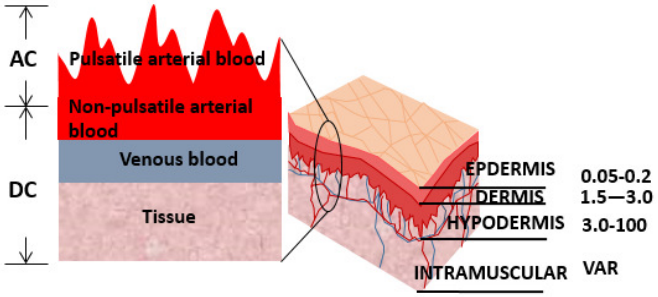

Fig. 3 Light absorption diagram and the AC and DC components of the signal corresponding to the pulsatile arterial, non-pulsatile arterial, venous blood and tissue information

To quantify tissue oxygenation, instead of capturing the pulsatile arterial blood flow, the Hamlyn StO_2 sensor is designed to capture the non-pulsatile arterial and venous blood flow. Fig. 3 illustrates the light absorption signal of skin tissue which contains pulsatile arterial blood, non-pulsatile arterial blood, venous blood and tissue information. Pulsatile and non-pulsatile blood flows are referred as AC and DC components in the signal. When the blood flow is blocked by a pressure cuff, the AC signal component will be dampened, as shown in Fig. 4.

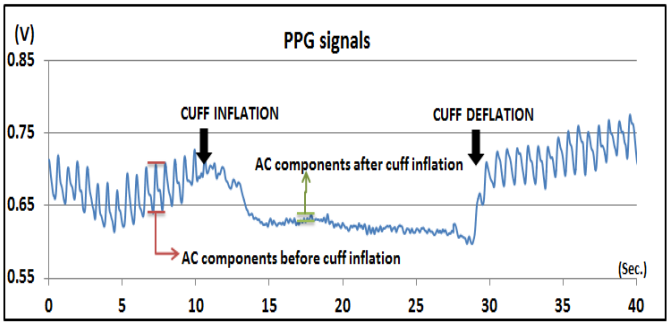

Fig. 4 Presence of pulsatile flow detected by the Hamlyn StO2 during supra-systolic cuff inflation

B. Active in-vitro Phantom Design for Sensor Calibration

To understand the tissue perfusion and optimize the design of the StO_2 sensor, experiments were designed using the tissue phantom and a healthy subject forearm ischemia model. Passive and active phantoms were designed and developed to study the spectral responses to fluid flow (blood flow) and hemodynamics in skin tissue.

Fig. 3 shows the layers of tissue from skin surface to deep musculature. It is not feasible to study tissue hemodynamics on human subjects and no such tissue phantom model is available. As such, we designed and developed a novel tissue phantom model to emulate different layers and vascular structures of subcutaneous tissue in order to study the light penetration and scattering on specific tissue layers. The optimal LED power and distance between the light source and photodiode can then be determined by analyzing the signal responses with regard to the

tissue depth.

Thus far, very few simulators have been proposed either in academic or commercial settings. The platform presented in [28] is a simulator designed for calibrating Sp(a)O_2 sensors and that of [29] is a phantom built with several disc layers to evaluate the light property/scattering in different disc layers for fiber-optics. A non-invasive haemoglobin measurement using NIR spectroscopy and PPG in blood components was carried out using a human blood model in [30]. Neither of these considered (1) the thickness of the skin (2) the diameter of the vessels or (3) the color difference in oxygenated and deoxygenated blood.

The first passive phantom shown in Fig. 5(A) was developed in the laboratory to study the sensory responses to discrete blood flow and synthetic blood with different colors. A silicone tube was chosen with an average diameter of 2.0mm/3.0mm (inner /outer diameters) to emulate a typical radial artery [31]. The silicone skin was made using the Nusil MED-4211 silicone elastomer with a recommended mix ratio of 10:1 (Part A: Part B) by weight and a small amount of skin-colored dye (Silc Pig™ Flesh PMS 488C, the color spectrum was close to 590nm). The synthetic vessel ran underneath the skin of three different thicknesses: 0.1mm, 3.0mm and 5.0mm, as shown in Fig. 5(B), emulating the blood vessels in different layers of skin tissue.

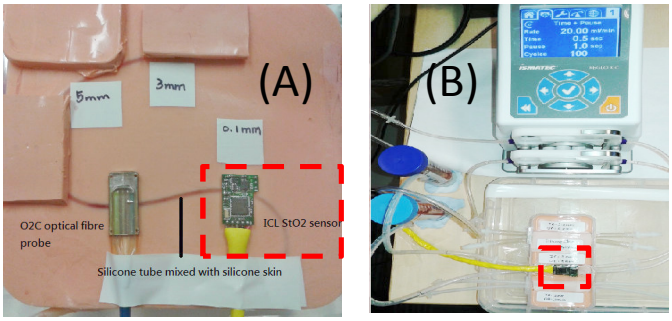

Fig. 5 Blood flow measurement using the phantoms (A) O2C probe and the Hamlyn StO2 sensor placed on passive phantom [24] (B)Active phantom and Hamlyn StO2 sensor placement

Venous thrombosis is one of the major causes of flap failure. A typical PPG sensor is designed mainly for detecting arterial blood flow. We designed our phantom to include both arterial and venous blood. Because arterial and venous blood have different visible absorption properties (colors), two pantone color codes [32], PMS1795C (arterial) and PMS 1815C (venous), were used to emulate venous and arterial blood. Fig. 6 shows the arterial and venous synthetic blood used in the phantoms. To test the phantom and validate the proposed StO_2 sensor, the O2C optical fiber probe and the Hamlyn StO_2 sensor were both placed side-by-side on top of the synthetic tissue (as shown in Fig. 5(A)), and synthetic blood was then manually injected through the vessels of our first passive phantom [24].

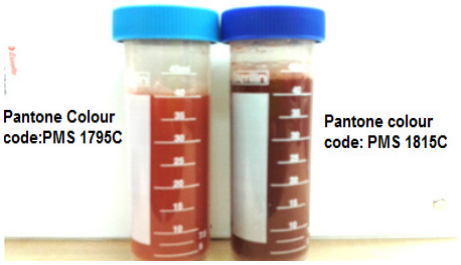

Fig. 6 Pantone color codes of two different synthetic blood for both passive and active phantom settings emulating the arterial (left) and venous blood (right) [24]

To simulate tissue hemodynamic with different diameters of vessels, an active phantom (Fig. 5(B)) was designed and developed. It was built by mixing a ratio 10:1(weights) of a rapid heat cure SYLARD 184 silicone elastomer with a small amount of skin-colored dye. The phantom was left in a desiccator connected to a vacuum pump for an hour-long degasification process before heat curing in an oven. The phantom was developed with three different inner/outer diameter (ID/OD) silicone tube pairs to emulate the different sizes of blood vessels in a typical skin tissue (as illustrated in Fig. 7). Each pair had two inputs and two outputs. [Pair I: 3.2mm/6.0mm (ID/OD), Pair II: 3.0mm/5.0mm (ID/OD), Pair III: 2.0mm/ 3.0mm (ID/OD)]. A silicone skin (The Chamberlain group) with 1.5mm thickness was cut into several pieces to cover up the phantom to evaluate the signal attenuation. A three-channel bi-directional flow speed control pump was connected between the fluid containers and the synthetic skin/vessel phantom. The pump drains the synthetic blood from two containers and then pushes it through the skin phantom simulating the pulsatile flow in a skin tissue. Each channel can be set to different flow rates, flow and pause time individually to simulate different scenarios and patterns.

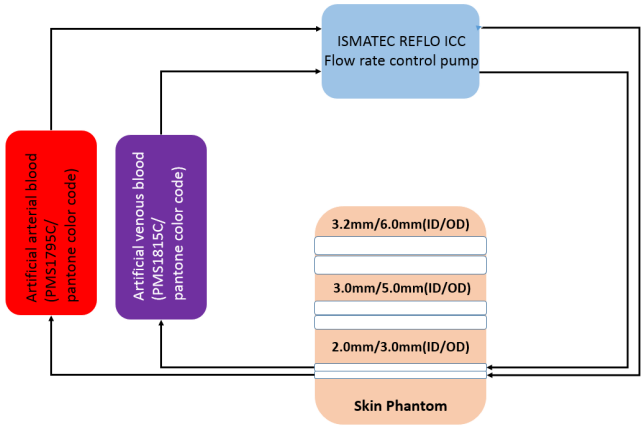

Fig. 7 Block diagram of the *in-vitro* active phantom

By using the *in-vitro* active phantom, SpO_2/SaO_2 sensors can be validated by measuring the absorption ratio of the two wavelength light sources as shown in Eq.5 [33].

$$R = K \times \frac{(AC_{red} / DC_{red})}{(AC_{IR} / DC_{IR})} \quad (5)$$

where K is considered as a constant value for validation. The equation consists of pulsatile (AC) and non-pulsatile (DC) components in two different wavelengths.

Following the empirical relationship between Sp(a)O_2 and the absorption ratio of the two LEDs (as shown in Fig. 8) as estimated by [34], Sp(a)O_2 as a percentage can be calculated using the following Eq. 6,

$$Sp(a)O_2\% = a - b \times R \quad (6)$$

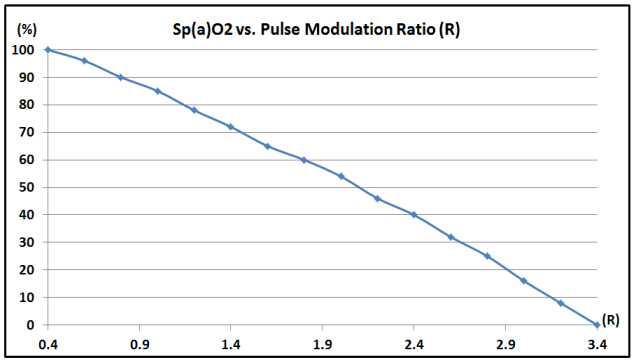

Fig. 8 Empirical relationship between the arterial Sp(a)O_2 and absorption ratio - data reproduced from [34]

To validate the proposed active phantom, a conventional medical grade oximeter (Nellcor N-95 Oximeter) was used. The flow and pause times were adjusted to 0.5 seconds and 1 second respectively in order to meet the minimum data collection specification of BPM (beat per minute) of the Nellcor N-95 Oximeter. Fig. 11(a) and (b) shows the results obtained by the Nellcor N-95 reflective sensor and the Hamlyn SpO_2 (660nm/940nm) sensor using the phantom. As the absorption ratio was 1, the expected SpO_2 readings should be 85%, and both the Nellcor and Hamlyn SpO_2 sensors obtained almost the same expected readings of 85.3±0.4% and 84.7±0.3% respectively. This demonstrates the feasibility of using the proposed active phantom for validating an SpO_2 sensor.

C. *Validation with a Forearm Ischemic Model*

In addition to validating the sensor using the proposed phantom, a healthy subject study was conducted to validate the feasibility and reliability of using the proposed StO_2 sensor in quantifying tissue viability. A pressure cuff forearm ischemia model was designed to compare the Hamlyn StO_2 sensor with the reference equipment (O2C). In the study, five healthy subjects were recruited locally. Written informed consent was gained in line with ethical approval granted by the NHS South East London Research Ethics Committee in December 2010 (10/H0808/124). After measuring the subject's blood pressure using a Sphygmomanometer, subjects were asked to sit with their left arm resting on a table as shown in Fig. 9.

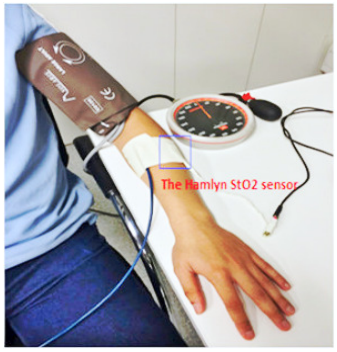

Fig. 9 Experiment set up – sensors are attached onto the forearm and a pressure cuff is wrapped around the upper arm

A brachial pressure cuff was then applied to the upper arm of the subject, and the Hamlyn StO_2 sensor and O2C probe were placed on the forearm parallel to each other longitudinally. An opaque adhesive dressing was applied to stabilize the sensors and limit the influence of ambient light. To emulate the deoxygenation conditions, a pressure cuff inflation protocol was designed to produce consistent, incremental reductions in tissue oxygen of the forearm. The first inflation lasted 150 seconds at a sub-diastolic pressure to block venous return from the arm but allow arterial inflow, simulating venous congestion. The next 5 inflations were supra-systolic for 30, 60, 90, 120 and 150 seconds, to block all blood flow to and from the arm, causing ischemia (shown in Fig. 13). In between each inflation episode, a resting period was taken to ensure that the O2C readings return to the baseline.

III. RESULTS

A. *Sensor Performance and Active Phantom Results*

The Hamlyn StO_2 sensor is designed for low power and continuous measurement of tissue oxygen saturation. The rail voltage of the system is 3V and the average current consumption is 2.2mA with a 1 KHz sampling rate. To validate the sensor, a simulated study was conducted to compare the proposed sensor with the O2C machine using the new proposed phantoms. Two different color synthetic bloods were injected into the phantom to mimic the arterial and venous flow through the tissue flap. Fig. 10 shows the sensor readings from the simulated study. The grey and green rectangles in the graph highlight the sensor data obtained when the synthetic blood with pantone color code: PMS 1795C (i.e. arterial blood) and PMS 1815C (i.e. venous blood) was injected into the phantom respectively.

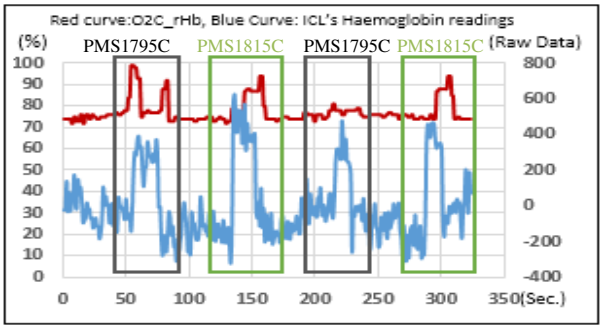

Fig. 10 Hemoglobin changes upon injection of two different color fluids into phantom: Blue signal: The Hamlyn StO_2 hemoglobin readings, Red signal: relative hemoglobin readings from O2C machine.

The blue signal in Fig. 10 is the hemoglobin data captured by the proposed StO_2 sensor, and the signal in red is the data captured by the O2C machine. As shown in Fig.10, both sensors can capture the synthetic blood flow and the variation of hemoglobin emulated with the proposed vascular phantom. It can be seen that different color synthetic blood will lead to very different signal amplitudes, as highlighted in Fig.10. It is less significant from the sensor signal of the O2C machine because (1) The O2C probe is insensitive with the fine silicone tube we used (~2mmOD/1mm ID) and (2) the O2C probe measures the relative hemoglobin of a human body so it can be relatively small compare to the StO_2 sensor readings.

Fig.11 (a) and (b) shows the SpO_2 readings obtained from the Hamlyn SpO_2 sensor and the Nellcor N-95 sensor using an active phantom.

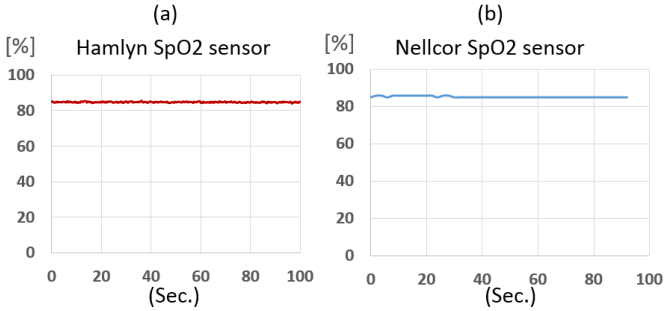

Fig. 11 a) SpO_2% (84.7±0.3%) obtained from the Hamlyn SpO_2 sensor (660nm/940nm), and (b) $Sp(a)O_2$ (85.3±0.4%) data collected from Nellcor N-95 on the active phantom

Fig. 12 shows the readings captured by the O2C machine on the active phantom. The top 2 figures are the fluid flow readings (P1S- superficial skin) and (P1D-deep skin or adipose tissue) from depth ~1mm and 4mm. The two blue rectangles marked with label 1 in Fig.12 highlight the readings obtained when the flow rate and pulse time of the phantom were set to 23ml/min. and 1 sec/1 sec drain/pulse time respectively. It can be seen that the readings are very different from those obtained when three different flow rates and pulse times were set (as highlighted by the rectangle labelled with 2 in Fig. 12).

The relative hemoglobin reading (Fig. 12 third figure) is slightly changed due to the variations in the flow rates and pulse times and oxygen saturation reading (Fig. 12 bottom figure) remains constant as there is no physiological oxygen transport in the silicone phantom.

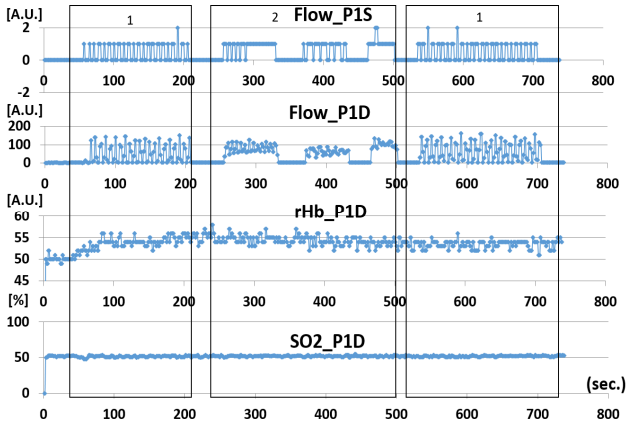

Fig. 12 Readings from the O2C machine with the active phantom: (Top) Fluid flow readings from P1S- superficial skin, (Second) fluid flow readings from P1D-deep skin or adipose tissue, (Third) the relative hemoglobin reading from P1D, and (Bottom) the oxygen saturation obtained from P1D

B. Results with healthy subject Forearm Ischemia Model

In addition to the simulated study using the phantom, a healthy subject study was conducted to assess the performance of the Hamlyn StO_2 sensor. Five healthy subjects were recruited in the study and the ischemia model was used. Fig. 13 shows the readings obtained from O2C and the Hamlyn StO_2 sensor where incremental pressures were applied using the pressure cuff to emulate ischemic conditions. As shown in Fig.14, the reading from the StO_2 sensor was significantly correlated with the O2C reading with Spearman's rank correlation of r= 0.672, $p < 0.001$. The correlation between the two sensors is shown in Fig. 14 signal obtained from the proposed Hamlyn StO2 sensor is similar to the O2C machine but not as precise, this is mainly due to its light weight and low-cost wearable design.

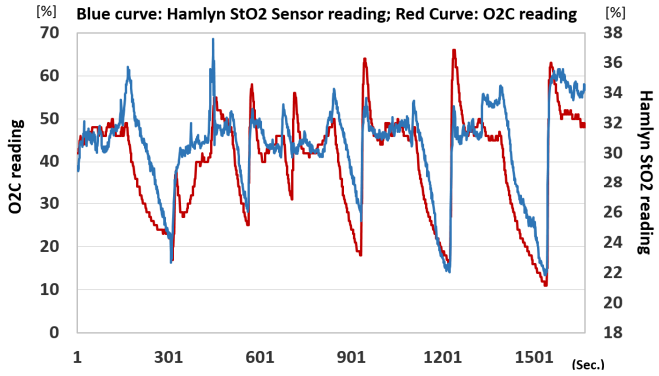

Fig. 13 StO2 readings from the O2C machine (red) and the Hamlyn StO_2 sensor (blue)

Incremental increases in cuff inflation resulted in a linear increase in deoxygenation readings from both O2C and the Hamlyn StO_2 sensors, with significant differences recorded on consecutive inflations ($p < 0.05$), as shown in Fig.15.

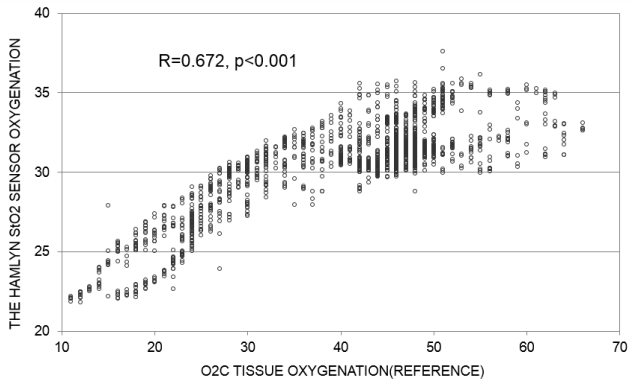

Fig. 14 Correlation between StO_2 readings from Hamlyn StO_2 sensor and the standard O2C machine

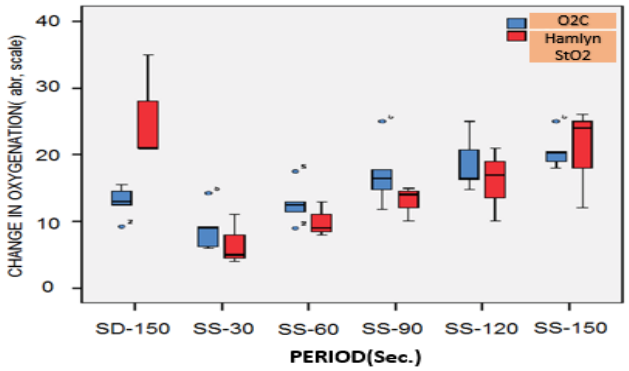

Fig. 15 Changes in tissue oxygenation values during cuff inflation protocol for optical sensor and O2C

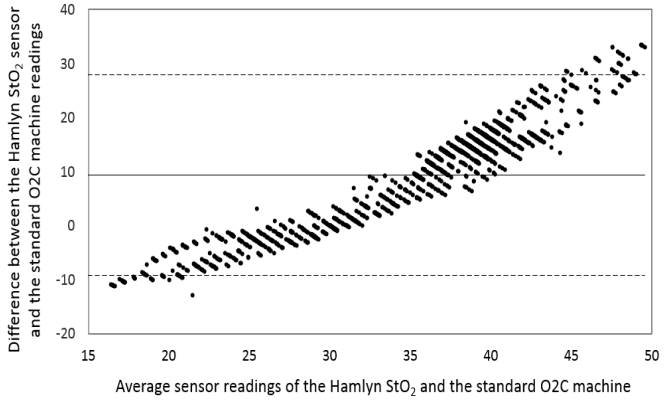

Fig.16 A Bland-Altman plot between StO2 readings from Hamlyn StO2 sensor and the standard O2C machine

The standard deviation of Bland-Altman plot (Fig.16) shows two individual measurements of the Hamlyn StO_2 sensor and the O2C machine.

IV. Conclusion and Discussion

Large soft tissue defects often can only be reconstructed by tissue grafts from distant locations (free flap), for example using the abdominal skin and fat to reconstruct a breast post-mastectomy. Intensive post-operative monitoring is essential to capture any sign of flap failure due to compromised vascular anastomosis. Early detection can significantly improve the chances of salvaging a failing tissue flap.

Temperature [20], microdialysis [21], laser Doppler [35], near infrared spectroscopy [22], and implantable Doppler [23] have been proposed for early detection of flap failure. However, the uptake in the National Health Service has been slow mainly due to the practical challenges including high up-front expenditure, complex and time-consuming data processing and interpretation, and lack of infrastructure to support an updated post-operative care paradigm.

In practice, flap failure and salvage rates differ considerably between units, which would underpin the cost-effectiveness of additional flap monitoring techniques. Should the implementation of a technique be such that the cost-effectiveness was neutral (as it may be in a specialist center), there are other potential gains. For patients, this may mean the avoidance of further surgery, tissue loss, and the stress on top of the current scenario of cancer or trauma. For surgeons, continuous monitoring with data transmission may provide peace of mind after hours, and might lead to more challenging cases being attempted.

In this paper, we presented a low power wearable StO_2 sensor, and demonstrated its feasibility in continuous monitoring of tissue viability after free autologous tissue transfer. To determine the optimal wavelength and optimize the power consumption of the sensor, *in-vitro* passive and active phantoms were designed and developed providing a controlled test bed for detailed analysis of light scattering properties, penetration depth, and other spectral responses. These test beds also enabled the simulation of arterial and venous blood flow (using different colored fluid), and from the experiment we demonstrated that the oxygenated and deoxygenated blood can be differentiated by using the proposed Hamlyn StO_2 sensor. Promising results were obtained from using both passive and active phantoms in the experiments. Apart from differentiating venous and artery blood, the continuously closed-loop active phantom can be used for SpO_2 sensor validation. It can provide a unique setting to simulate different conditions for SpO_2 validation and demonstration. However, a capillary silicone tissue bed is yet to be developed and integrated into the phantom to simulate oxygenation for calibrating the Hamlyn StO_2 sensors.

A pressure cuff forearm ischemia model was designed to validate the Hamlyn StO_2 sensor by comparing it with a reference equipment (O2C). Significant correlation was found from the readings of both sensors when different deoxygenation conditions were simulated by incrementally applying pressure on the subjects' upper arm. This demonstrates the potential of the sensor in detecting ischemia or flap failure and also quantifying the deoxygenation processes in human tissue. The study has been extended to include more healthy subjects and a pilot clinical study has been planned to validate the sensor to demonstrate the feasibly and reliability of the sensor for clinical

use.

Further clinical applications of the Hamlyn StO_2 include tissue monitoring in the setting of peripheral vascular insufficiency, such as in diabetic foot or intermittent claudication. Access to a pervasive methods of monitoring would reduce the current constraints that prevent the implementation of proactive and preventive interventions.

ACKNOWLEDGMENTS

This research work is sponsored by the NIHR Imperial BRC project - a reflective photoplethysmographic plaster for monitoring soft tissue viability after free autologous tissue flap transfer, and the EPSRC (EP/L014149/1) Smart Sensing for Surgery project. Authors would like to thank Mr Shehan Hettiaratchy, Imperial College Healthcare NHS Trust, and Dr. Daniel Leff, Department of Surgery, Imperial College London for their support to this project.

REFERENCES

[1] G.-Z. Yang and M. Yacoub, "Body sensor networks",Springer, 2006.

[2] C. M. Chen, K. Onyenso, G.-Z. Yang, and B. Lo, "A multi-sensor platform for monitoring diabetic peripheral neuropathy," in *Wearable and Implantable Body Sensor Networks (BSN), 2015 IEEE 12th International Conference on*, 2015, pp. 1-6: IEEE.

[3] L. Wang, B. P. Lo, and G.-Z. Yang, "Multichannel reflective PPG earpiece sensor with passive motion cancellation," *Biomedical Circuits and Systems, IEEE Transactions on,* vol. 1, no. 4, pp. 235-241, 2007.

[4] B. P. L. Lo, H. Ip, and G.-Z. Yang, "Transforming Health Care - Body sensor networks, wearables and the Internet of Things," *IEEE Pulse* Jan 2016 2016.

[5] J. Nanchahal, S. Nayagam, U. Khan, C. Moran, S. Barrett, F. Sanderson, I. Pallister, and H. Liang,"Standards for the management of Open Fractures of the Lower Limb - a short guide", ed: *British Association of Plastic Reconstructive and Aesthetic Surgeons (BAPRAS)*, PP.22,2009

[6] J. H. Yueh *et al.*, "Patient satisfaction in postmastectomy breast reconstruction: a comparative evaluation of DIEP, TRAM, latissimus flap, and implant techniques," *Plastic and reconstructive surgery,* vol. 125, no. 6, pp. 1585-1595, 2010.

[7] R. A. Agha, B. Gundogan, A. J. Fowler, T. W. Bragg, and D. P. Orgill, "The efficacy of the Cook-Swartz implantable Doppler in the detection of free-flap compromise: a systematic review protocol," *BMJ open,* vol. 4, no. 3, p. e004253, 2014.

[8] B. Creech and S. Miller, "Evaluation of circulation in skin flaps," in *Skin flaps*, W. Grabb and M. Myers, Eds. Boston: Little, Brown, 1975.

[9] J. M. Smit, C. J. Zeebregts, R. Acosta, and P. M. Werker, "Advancements in free flap monitoring in the last decade: a critical review," *Plastic and reconstructive surgery,* vol. 125, no. 1, pp. 177-185, 2010.

[10] Perimed. (2016). *TcpO2 product information*. Available: http://www.perimed-instruments.com/support/theory/tcp02

[11] G. Dowd, K. Linge, and G. Bentley, "Measurement of transcutaneous oxygen pressure in normal and ischaemic skin," *Journal of Bone & Joint Surgery, British Volume,* vol. 65, no. 1, pp. 79-83, 1983.

[12] R. Wütschert and H. Bounameaux, "Determination of amputation level in ischemic limbs: reappraisal of the measurement of TcPO2," *Diabetes Care,* vol. 20, no. 8, pp. 1315-1318, 1997.

[13] D. Marsden, M. Chiu, F. Paky, and P. Helms, "Transcutaneous oxygen and carbon dioxide monitoring in intensive care," *Archives of disease in childhood,* vol. 60, no. 12, pp. 1158-1161, 1985.

[14] D. R. Hargroves, R. C. Tallis, V. M. Pomeroy, and A. Bhalla, "Near-infrared spectroscopy in stroke: from research to clinical practice," *Stroke,* vol. 35, no. 11, pp. 2430-2431, 2004.

[15] J. Miner, R. Nelson, and L. Hayden, "The effect of near infrared spectroscopy monitoring on the treatment of patients presenting to the emergency department in shock," *Crit. Care Med.,* vol. 38, p. S861, 2010.

[16] S. GROSEK, M. ZNIDARSIC ERZEN, M. JELIC, A. GORNIK, and M. PODBREGAR, "Near infrared spectroscopy tissue oxygenation in infants with bronchiolitis during mechanical ventilation and spontaneous breathing," *Signa Vitae,* vol. 9, no. 2, pp. 15-24, 2014.

[17] S. G. Sagraves *et al.*, "Tissue oxygenation monitoring in the field: a new EMS vital sign," *Journal of Trauma and Acute Care Surgery,* vol. 67, no. 3, pp. 441-444, 2009.

[18] F. Hölzle, D. J. Loeffelbein, D. Nolte, and K.-D. Wolff, "Free flap monitoring using simultaneous non-invasive laser Doppler flowmetry and tissue spectrophotometry," *Journal of cranio-maxillofacial surgery,* vol. 34, no. 1, pp. 25-33, 2006.

[19] L. M. GmbH. (2016). *O2C (oxygen to see)*. Available: http://www.lea.de/eng/indexe.html

[20] R. K. Khouri and W. W. Shaw, "Monitoring of Free Flaps with Surface-Temperature Recordings: Is It Reliable?," *Plastic and reconstructive surgery,* vol. 89, no. 3, pp. 495-499, 1992.

[21] C. Mourouzis, R. Anand, J. R. Bowden, and P. A. Brennan, "Microdialysis: Use in the assessment of a buried bone-only fibular free flap," *Plastic and reconstructive surgery,* vol. 120, no. 5, pp. 1363-1366, 2007.

[22] M. H. Steele, "Three-year experience using near infrared spectroscopy tissue oximetry monitoring of free tissue transfers," *Annals of plastic surgery,* vol. 66, no. 5, pp. 540-545, 2011.

[23] T. Poder and P.-H. Fortier, "Implantable Doppler in monitoring free flaps: a cost-effectiveness analysis based on a systematic review of the literature," *European annals of otorhinolaryngology, head and neck diseases,* vol. 130, no. 2, pp. 79-85, 2013.

[24] C. M. Chen, R. Kwasnicki, B. Lo, and G. -Z. Yang, "Wearable Tissue Oxygenation Monitoring Sensor and a Forearm Vascular Phantom Design for Data Validation," in *Wearable and Implantable Body Sensor Networks (BSN), 2014 11th International Conference on*, 2014, pp. 64-68.

[25] J. A. Patterson and G.-Z. Yang, "Ratiometric artifact reduction in low power reflective photoplethysmography," *Biomedical Circuits and Systems, IEEE Transactions on,* vol. 5, no. 4, pp. 330-338, 2011.

[26] P. D. Mannheimer, J. Cascini, M. E. Fein, and S. L. Nierlich, "Wavelength selection for low-saturation pulse oximetry," *Biomedical Engineering, IEEE Transactions on,* vol. 44, no. 3, pp. 148-158, 1997.

[27] W. Zijlstra, A. Buursma, and W. Meeuwsen-Van der Roest, "Absorption spectra of human fetal and adult oxyhemoglobin, de-oxyhemoglobin, carboxyhemoglobin, and methemoglobin," *Clinical chemistry,* vol. 37, no. 9, pp. 1633-1638, 1991.

[28] V. Rybynok, J. May, K. Budidha, and P. Kyriacou, "Design and development of a novel multi-channel photoplethysmographic research system," in *Point-of-Care Healthcare Technologies (PHT), 2013 IEEE*, 2013, pp. 267-270: IEEE.

[29] M. Larsson, W. Steenbergen, and T. Stro, "Influence of optical properties and fiber separation on laser Doppler flowmetry," *Journal of Biomedical Optics,* vol. 7, no. 2, pp. 236-243, 2002.

[30] J. Kraitl, D. Klinger, D. Fricke, U. Timm, and H. Ewald, "Non-invasive Measurement of Blood components Sensing for an In-Vivo Heamoglobin Measurement", S.C. Mukhopadhyay et al.(ed) in *Advancement in Sensing Technology*, Springer-Verlag Berlin Heidelberg, SSMI 1, pp. 237-262, 2013

[31] T. Ashraf, Z. Panhwar, S. Habib, M. A. Memon, F. Shamsi, and J. Arif, "Size of radial and ulnar artery in local population," *JPMA-Journal of the Pakistan Medical Association,* vol. 60, no. 10, p. 817, 2010.

[32] A. Kienle, L.Lilge, I. A. Vitkin, M. S. Patterson, B. C. Wilson, R. Hibst and R. Steiner,"Why do veins appear blue?A new look at an old equation", *Applied Optics*, vol. 35, pp.1151-1160,1996

[33] Y. Mendelson, "Pulse oximetry: theory and applications for noninvasive monitoring," *Clinical chemistry,* vol. 38, no. 9, pp. 1601-1607, 1992.

[34] J. G. Webster, *Design of pulse oximeters*. CRC Press, 1997.

[35] M. D. Stern *et al.*, "Continuous measurement of tissue blood flow by laser-Doppler spectroscopy," *American Journal of Physiology-Heart and Circulatory Physiology,* vol. 232, no. 4, pp. H441-H448, 1977.